Journal of Power Sources 195 (2010) 5660–5665

Contents lists available at ScienceDirect

Journal of Power Sources

journal homepage: www.elsevier.com/locate/jpowsour

Structure and conductivity of yttria-stabilized zirconia co-doped with Gd_2O_3: A combined experimental and molecular dynamics study

X. Xie [a,b,*], R.V. Kumar [a], J. Sun [b], L.J. Henson [a]

[a] Department of Materials Science and Metallurgy, University of Cambridge, Cambridge CB2 3QZ, United Kingdom
[b] Department of Inorganic Nonmetallic Materials, University of Science and Technology Beijing, Beijing 100083, PR China

ARTICLE INFO

Article history:
Received 3 January 2010
Received in revised form 9 March 2010
Accepted 14 March 2010
Available online 20 March 2010

Keywords:
Yttria-stabilized zirconia
Co-doping
Gadolinia
Molecular dynamics
Symmetry
Conductivity

ABSTRACT

Yttria-stabilized zirconia (YSZ) samples co-doped with Gd_2O_3 in the range 0–4 mol% were prepared and their ionic conductivities were investigated as a function of Gd_2O_3 concentration by impedance spectroscopy. Bulk conductivity of 8 mol% YSZ electrolyte at temperatures <726 K was enhanced by Gd_2O_3 co-doping up to levels of 2 mol%, while the total conductivity maxima was achieved at a composition of 2 mol% at temperatures not over than 623 K. Based on analyses of results from both molecular dynamics calculation and experimental investigation, the achievement of higher ordered cubic symmetry is suggested as an explanation for the enhanced conductivity at a relatively low temperature arising from co-doping YSZ with Gd_2O_3.

1. Introduction

As a practical way to ease up the crisis of energy and environment, solid oxide fuel cells (SOFCs) can convert the chemical energy in a fuel to electric energy directly with high efficiency and low levels of pollution. It is well known that zirconia can exhibit high ionic conductivity when doped with yttria, which increases the concentration of oxygen vacancies by aliovalent substitution of Zr^{4+} with Y^{3+}. Doping in this manner also stabilizes the ionically conductive cubic fluorite phase of zirconia relevant to the operating temperatures of a fuel cell. Yttria-stabilized zirconia (YSZ) typically at 8 mol% yttria, is most common material used in SOFCs. YSZ's success can be attributed to its many advantages over other candidates, such as acceptable ionic conduction at $T > 1250$ K, a wide range of composition for phase stability, high resistance to chemical reduction, reasonable mechanical strength and relatively low-cost. The major limitation arises from the need to operate at relatively high temperatures of around 1250–1300 K to achieve adequate conduction. High temperatures preclude the use of low-cost metals for the interconnect component of the fuel cell stack but also increase the likelihood of thermal shock induced cracks. These challenges have hampered progress in YSZ becoming more widely available for commercial fuel cell applications.

There are a number of approaches that have been considered for enhancing ionic conductivity of the solid electrolyte with a view to lowering the operating temperature of SOFCs [1–6]. The key is to minimize the impedance of cell by enhancing the ionic conductivity at lower temperatures while simultaneously minimizing any electronic conduction to avoid currents leaking. Further optimizations in the binary YSZ system has resulted in only minor improvements. Doping has been considered as a convenient and potentially effectual method to improve the properties of the electrolyte materials through increasing concentration of mobile vacancies or by scavenging of grain boundary to minimize interfacial resistance. Homogeneous co-doping, with Sc, to give a ternary system of Y_2O_3–Sc_2O_3–ZrO_2 has shown some promise for enhancing the ionic conductivity of zirconia [7]. However, scandia is expensive [8]. To open up new avenues in solving the challenges facing application, co-doping has shown some promise for improving the ionic conductivity further [5,9,10].

Gd_2O_3 is well known as a dopant oxide applied in ceria-based systems. According to calculations from lattice simulation embodied GULP code, Gd^{3+} has a favorable dopant solution energy at near 0 eV and a ionic radius similar to that of Y^{3+}(1.019 Å for Y^{3+} vs 1.053 Å for Gd^{3+}) [11]. However, to our knowledge, there are only scattered previous research reports focusing on zirconia-based electrolyte co-doped with both Gd_2O_3 and Y_2O_3. Kan et al. [12] analyzed the effect of Gd_2O_3 doping content on YSZ materials prop-

* Corresponding author at: Department of Materials Science and Metallurgy, University of Cambridge, Pembroke Street, Cambridge CB2 3QZ, United Kingdom. Tel.: +44 1223 334327; fax: +44 1223 334467.
E-mail address: xx769@cam.ac.uk (X. Xie).

0378-7753/$ – see front matter © 2010 Elsevier B.V. All rights reserved.
doi:10.1016/j.jpowsour.2010.03.054

Table 1
Potential coefficients employed in the MD simulation.

Interaction	A (eV)	ρ (Å)	C (eV Å^6)	Ref.
Zr^{4+}–O^{2-}	1024.6	0.376	0	[14–16]
Y^{3+}–O^{2-}	1325.6	0.3461	0	[14–16]
Gd^{3+}–O^{2-}	1336.8	0.3551	0	[15]
O^{2-}–O^{2-}	22764.3	0.149	27.88	[15]

erties and found that the conductivity can substantially increase with increasing Gd_2O_3 addition. However, the total amounts of both Y_2O_3 and Gd_2O_3 were varied and <8 mol% in their study, resulting in varying amounts of oxygen vacancy concentrations. The enhanced conductivity maybe caused by the increasing of oxygen vacancy because at 8 mol% doping level for yttria can achieve a maximum conductivity in YSZ binary system.

The aim of this work is focused on co-doping yttria-stabilized zirconia (YSZ) materials with Gd_2O_3 while maintaining a constant concentration of oxygen vacancy. The influence of doping on micro-structural and electrochemical properties of the electrolytes is discussed. In an attempt to determine the defect and transport properties of electrolyte materials, molecular dynamics simulations are performed to study the structure and conductivity in the YSZ using Buckingham potentials, which are particularly suited for probing ionic transport properties.

2. Experiment

High-purity 8 mol% yttria-stabilized zirconia powders and zirconia powders (TZ-8Y and TZ-0, Tosho Co., Ltd.) were used as the starting material. Stoichiometric amounts of Gd_2O_3 was introduced via a solution route of gadolinium nitrate ($Gd(NO_3)_3{\cdot}6H_2O$ 99%, Aldrich) for the composition range $(Gd_2O_3)_x(Y_2O_3)_{0.08-x}(ZrO_2)_{0.92}$, where x was varied from 0 to 0.04 and are represented as $Gd_yY(8-y)$, throughout this work, where $y = 100x$, represent the mol%. The mixed powders of TZ-8Y, TZ-0 and gadolinium nitrate with ethanol were ball milled in a plastic jar for 24 h and subsequently dried. Green YSZ (with Gd) cylindrical pellets of 20 mm diameter and 2–2.5 mm thickness were prepared by uniaxial pressing at 30 MPa. The specimens were sintered at 1450 °C for 4 h in air at a linear heating rate of 1.5 °C min^{-1} with a dwell time of 1 h at 700 °C for achieving nitrate decomposition. The relative densities of the sintered samples were measured by Archimedean principle. The results showed that very dense specimens (>99%) could be obtained by the above method. Phase identification of these sintered specimens was carried out using an X-ray diffractometer (Philips, PW1820) with CuKα radiation at 40 kV and 40 mA. Ionic conductivities were determined by an ac impedance analyzer (Solarton 1260 + 1286) in the frequency range 5 MHz to 1 Hz at temperatures 473–1023 K in air with silver paste electrodes.

The DL_POLY [13] code was used in this study to perform the molecular dynamics (MD) simulations. The Buckingham potentials supplemented with electrostatic terms (Eq. (1)) was adopted in the present MD simulations to study the molecular behavior of ionic and oxygen vacancy transport in YSZ and some other physical properties of the materials are also investigated. The potential parameters are summarized in Table 1, which was validated by comparing the experiment lattice constants with MD result [14]. The ensemble used imposed the conditions of constant number of ions, pressure and temperature (NPT):

$$V(r_{ij}) = A\exp\left(-\frac{r_{ij}}{\rho}\right) - \frac{C}{r_{ij}^6} + \frac{q_i q_j}{r_{ij}} \quad (1)$$

where A, ρ and C are parameters fitted to the experimental properties of the material, q_i is the charge of atom i and r_{ij} is the distances between atoms i and j. A is a measure of the interaction strength, ρ measures the distance over which the attractive force decrease and C is a measure for the repulsive force.

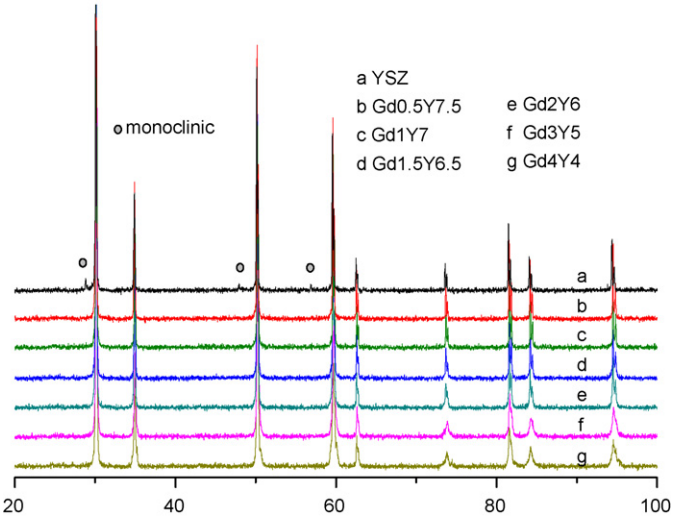

Fig. 1. XRD patterns taken from the sintered pellets of 8YSZ doped with varying Gd_2O_3 content.

According to the XRD pattern when YSZ is co-doped with Gd_2O_3 the solid electrolyte still has the fluorite-type cubic phase within the 0–4 mol% Gd_2O_3 content. A supercell consisting of 768 ions ($4\times4\times4$ unit cells) with 256 Zr and 512 O ions were generated based on the fluorite structure. Suitable number of Zr ions is replaced by Y (and Gd ions), while O ions equal to the half of Y (+Gd) are removed from supercell at random as suggested by the defect equation (Eq. (2)):

$$Y_2O_3 + 2Zr_{Zr}^{x} + O_O \rightarrow 2Y_{Zr}^{'} + V_{\ddot{O}} + 2ZrO_2 \quad (2)$$

Then, MD simulation was performed for 600 ps to deduce the simulated results under the desired condition, and up to 100 ps for ensemble equilibrium, with a step time of 5×10^{-4} ps.

After molecular dynamic simulation at different temperature, ionic diffusion coefficients were obtained from slope of the mean square displacement (MSD) and the radial distribution functions (RDF) were also calculated from the trajectories of the respective ions.

Based on the evaluation of the quality of the potentials employed, a simulation of 8YSZ co-doped by gadolinia was carried out as a function of Gd_2O_3 concentrations ranging from 0 mol% to 4 mol% at temperature ranging from 973 K to 1573 K. Results from the simulation are compared with experimental results.

3. Results and discussion

3.1. Microstructure analysis

The XRD patterns of 8YSZ doped with Gd_2O_3 in the range of 0–4 mol% are shown in Fig. 1. The results show that co-doping with Gd_2O_3 retains the cubic phase as in 8 mol% YSZ. There are also no obvious characteristic peaks of Gd_2O_3 presented in XRD diffractograms within the Gd_2O_3 content range used in this study. In contrast, the peaks located at around 28°, 47° and 57° of 8YSZ, corresponding to a small amount of monoclinic phase disappeared after Gd_2O_3 was introduced. The absence of monoclinic indicates that the cubic phase is stabilized.

As a corresponding analogue of XRD structure analysis in the molecular dynamic system, the pair radial distribution function (RDF) can be a useful way in order to describe how the density of surrounding structure varies as a function of the distance from a

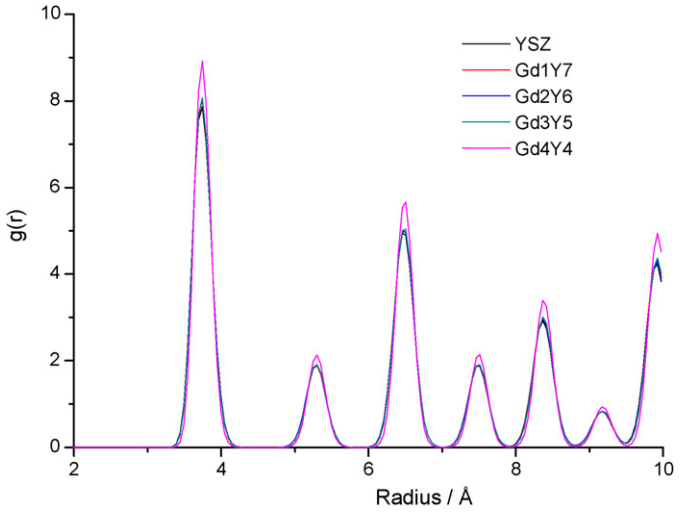

Fig. 2. Radial distribution functions for Zr–Zr with different Gd_2O_3 concentration at 973 K.

particular point, thus reflecting the structural information. In particular, the RDF, denoted by $g(r)$, can be calculated as:

$$g(r) = \frac{\langle N(r, \Delta r)\rangle}{(1/2)N\rho V(R, \Delta r)} \quad (3)$$

where $\langle N(r, \Delta r)\rangle$ indicates the number of atoms found within a spherical shell of $r + \Delta r$ averaged over time, and N and ρ refer to total number of atoms and system number density, respectively. V is the shell volume. Fig. 2 shows the RDF of the Zr–Zr vs radius with respect to different Gd_2O_3 concentration at 973 K. The superimposed pattern is similar to pure YSZ and the nearest cation–cation distances of Zr–Zr is almost equal, which indicating that the system maintains a cubic structure at different Gd concentrations. The RDF patterns of Zr–O, Gd–O and Y–O pairs for Gd2Y6 are plotted in Fig. 3. As seen in Fig. 3, the nearest cation–anion distances of Zr–O is shorter than Y–O and Gd–O. This is caused by a larger Coulombic interaction of tetravalent cation with O in comparison with the trivalent ions. It is found that the Gd–O distance is longer than the Y–O distance, which may be due to the fact that Gd^{3+} has a slightly larger radius than that of Y^{3+}. It also observed that the average coordination number of Gd (7.950), which is determined by integrating the RDF to the first minimum, is higher than that of Y (7.875) arising from a larger ionic radius of Gd and a greater preference for eightfold coordination. Therefore, an enhanced cubic symmetry on the surrounding anion sub-lattice is consistent with other reports [11,17]. Compared with the average coordination number Zr (7.714), the higher that of Gd and Y indicate that oxygen vacancies prefer to be located at the first nearest neighbor position with respect to Zr^{4+}, which is similar with the data for YSZ from nuclear magnetic resonance (NMR) monitoring [18].

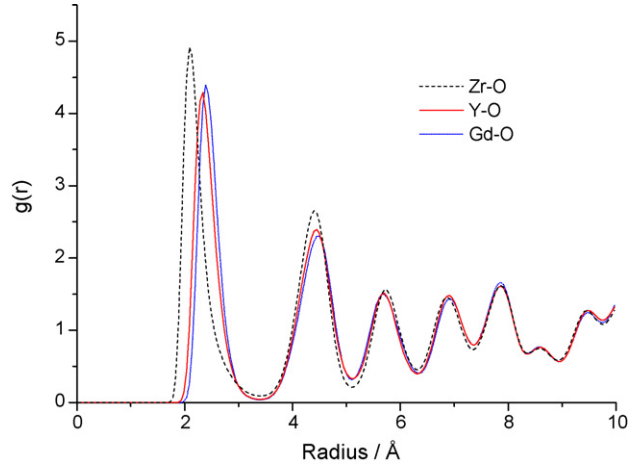

Fig. 3. Radial distribution functions for Zr–O, Y–O and Gd–O pairs in Gd2Y6 at 973 K.

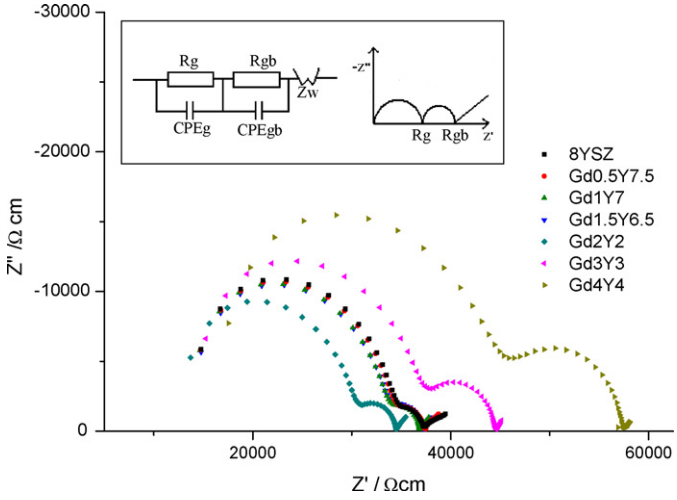

Fig. 4. Complex impedance spectra of YSZ co-doped Gd_2O_3 specimens at 623 K in air and schematic equivalent circuits and corresponding ac impedance response (R_g, R_{gb}, CPE_g, CPE_{gb} and Z_w represent grain bulk resistance, grain boundary resistance, constant phase element of grain, constant phase element of the grain boundary and Warburg impedance, respectively).

3.2. Diffusion and ionic conductivity

Fig. 4 shows a complex specific impedance plot of the YSZ samples co-doped with different Gd_2O_3 concentration at a temperature of 623 K. The brick model was employed to describe equivalent circuits for impedance spectroscopy of the polycrystalline electrolytes. As shown in the inset of Fig. 4, two independent semicircular arcs moving from high to low frequency correspond to the bulk and grain boundary resistance, and a diffusion-limited process leads to an impedance response (Warburg impedance, Zw) that appears as a straight line in the lower frequency range. The bulk conductivity (σ_b), apparent grain boundary conductivity (σ_{gb}^{app}) and total conductivity (σ_{tol}) can be calculated from $\sigma_b = L/AR_b$, $(\sigma_{gb}^{app}) = L/AR_{gb}^{app}$ and $\sigma_{tol} = L/AR_{total}$, where L and A are the thickness and cross-section area of specimens, respectively.

In Fig. 5, the bulk and apparent grain boundary conductivity of co-doped YSZ are both plotted as a function of mol% Gd_2O_3 at 573 K. As shown in Fig. 5, the addition of $\leq$2 mol% Gd_2O_3 increases the grain bulk conductivity of YSZ. According to interpretation from both experimental and MD simulations above, the symmetry of cubic structure was enhanced by replacing Y_2O_3 with Gd_2O_3. Generally, well ordered cubic structure in zirconia can lead to faster ionic transport. Thus the conductivity is increased with increasing Gd_2O_3 concentration, but only up to a limiting value of 2 mol%. The trend is reversed when more than 2 mol% Gd_2O_3 content is introduced. This decrease in conductivity may be attributed to difference in ionic size and cluster binding energies of Gd^{3+} and Y^{3+}. At higher concentrations, the larger ionic radius may be impeding the oxygen ion migration. The cluster binding energies for Gd^{3+}(−0.3 eV) are also stronger than Y^{3+}(−0.26 eV) [11], which can indicate greater difficulty in moving an oxygen vacancy. Therefore, diffusion in the bulk is slowed by co-doping Y_2O_3 with higher concentration of Gd_2O_3. It is found in Fig. 5 that the grain boundary conductivity also decreases with increasing Gd_2O_3 doping concentration, which

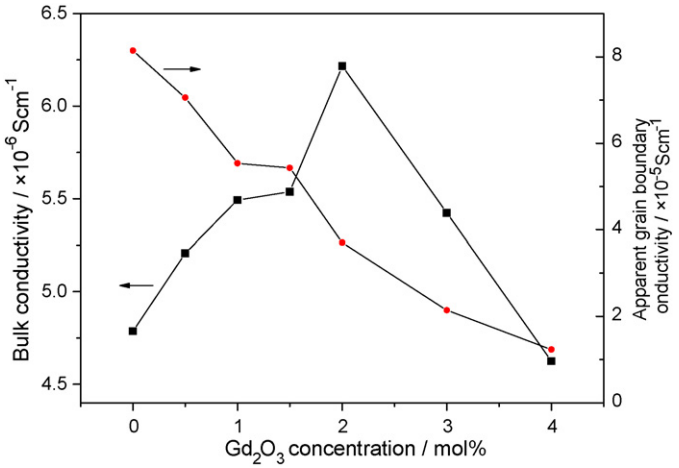

Fig. 5. The bulk conductivity and apparent grain boundary conductivity of the samples as a function of Gd_2O_3 doping levels at 473 K.

is an indication that Gd^{3+} can segregate into the grain boundary with increasing effect as concentration is increased. Partition of any Gd^{3+} cation into the grain boundary will lead to a decrease in the number of substituted Zr^{4+} cation in the lattice and thus reduce the amount of oxygen vacancy and lower the conductivity in the grain. The above combination of factors can therefore explain why a conductivity maximum is achieved on adding Gd_2O_3 to YSZ.

Fig. 6(a) and (b) displays the bulk and total conductivity data of specimens in an Arrhenius plot at 473–623 K, while the total conductivity data for 673–1023 K are shown in Fig. 7. Deriving from the slope shown in Fig. 6(a), Gd_2O_3 co-doped specimens had a higher bulk conductivity than 8YSZ only below the max temperature of 726 K, while the total conductivity maxima was achieved at a composition of 2 mol% at temperatures not over than 623 K (Figs. 6(b) and 7). In additional, the oxygen conductivity is normally expressed as follows:

$$\sigma T = A \ \exp\left(\frac{-E_a}{kT}\right) \tag{4}$$

where σ is the ionic conductivity, T is the absolute temperature, A pre-exponential constant, and E_a is the activation energy. The activation energy can be calculated from the slope of $\ln \sigma T$ vs $1/T$. It is shown in Fig. 8 that the activation energy of the bulk decreases with increasing Gd_2O_3 concentration. The decreasing for electrolyte was suggested as co-doping with Gd_2O_3 can improve cubic order of YSZ lattice, which provides a well structure for faster ionic transport thus decrease potential barrier for more easily overcoming. But the activation energy data for the grain boundary exhibit an increasing trend as Gd_2O_3 was increased (Fig. 8), which is relate to the phenomenon that the partition of any Gd^{3+} cation distributed in the grain boundary and blocked the pathway for oxygen anion migrating in the grain boundary.

The phenomenon of bulk conductivity affected by Gd_2O_3 co-doping is also studied with MD simulation. In particular, the conductivity of YSZ electrolyte can be expressed in terms of ionic diffusion of oxygen ions and the ionic self diffusion was determined from calculated mean square displacement (MSDs) as following:

$$\text{MSD} = < r_i^2(t) > = \frac{1}{N}\sum_{1}^{N}[r_i(t) - r_i(0)]^2 \tag{5}$$

Furthermore, the diffusion coefficient, D_i, then be derived from the MSD slope based on Eq. (4), where B is the Debye–Waller factor:

$$< r_i^2(t) > = 6D_i t + B \tag{6}$$

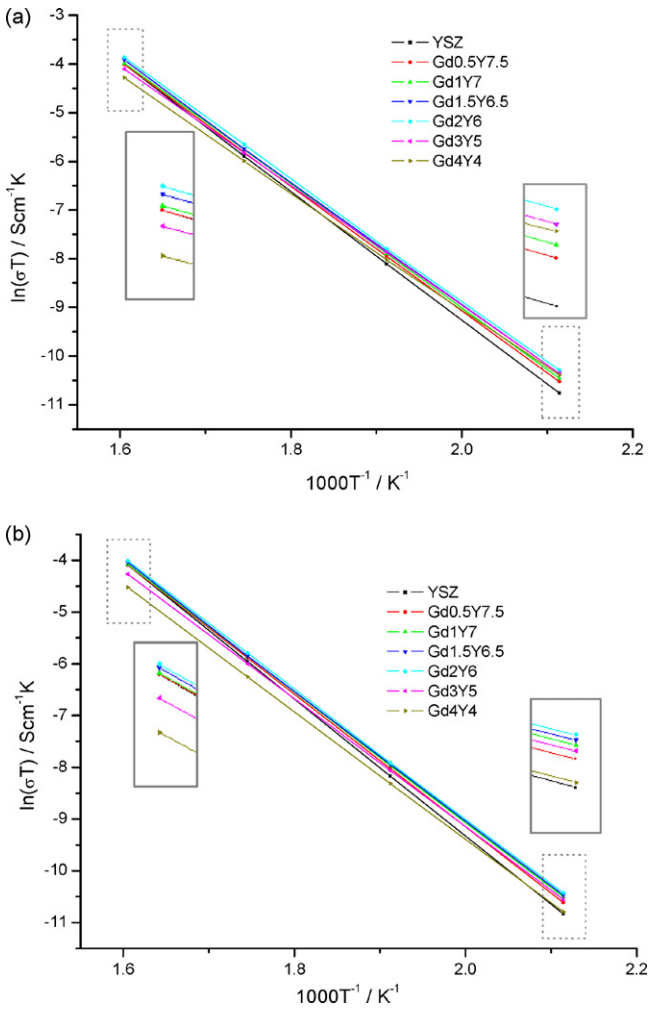

Fig. 6. The conductivity of the samples with various Gd_2O_3 concentrations for 473–623 K (a) bulk and (b) total.

Fig. 9 shows a typical plot from oxygen MSD results from Gd2Y6 molecular dynamic as a function of simulation time for each calculation at different temperature. It can be clearly seen that the mean square displacements of the oxygen increases linearly with the simulation time. Moreover, the slope of the MSD line increased

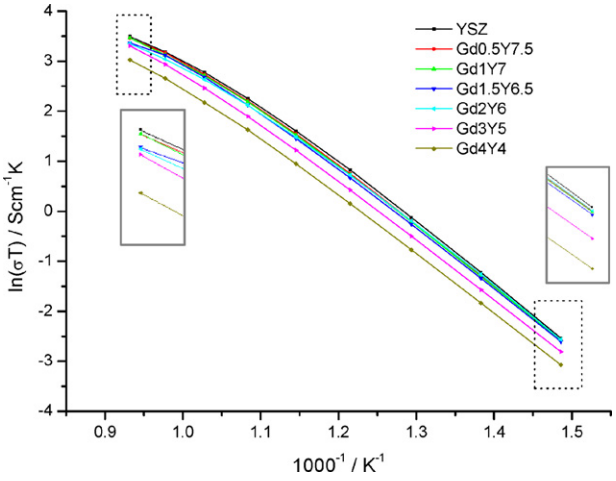

Fig. 7. The total conductivity of the samples with various Gd_2O_3 concentrations for 673–1073 K.

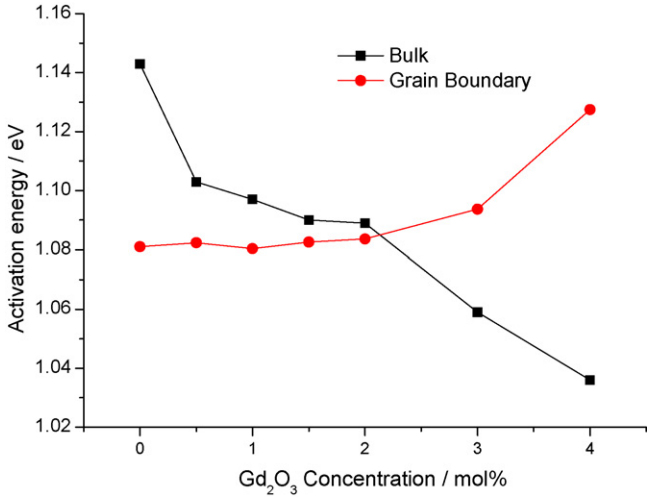

Fig. 8. The activation energy of electrolyte for bulk and grain boundary conductivity as a function of Gd_2O_3 concentration.

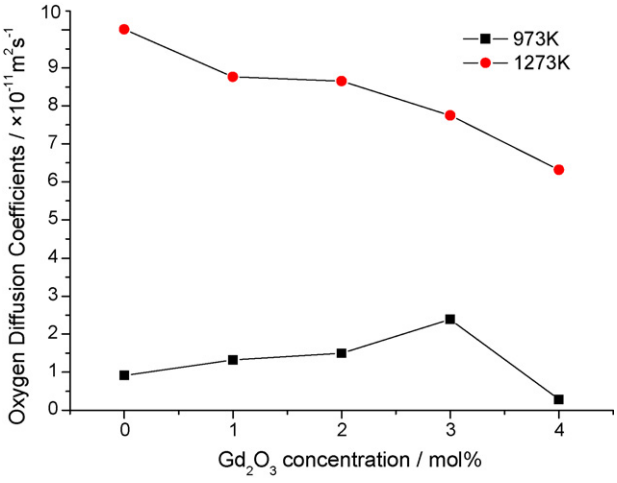

Fig. 11. Calculated oxygen diffusion coefficients from MD results at 973 K and 1273 K.

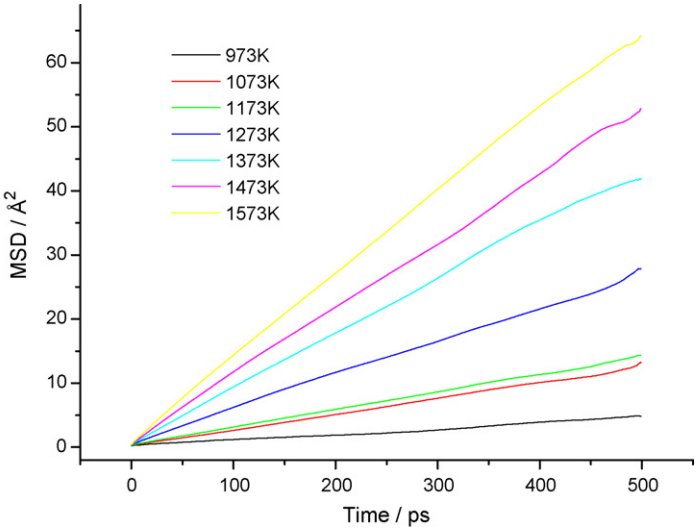

Fig. 9. MSDs of oxygen ions at different temperature in Gd2Y6 sample.

as temperature was ramped. The increasing value of MSD slope reflects more rapid oxygen transport at elevated temperatures, and thus enhanced ionic conductivity. After 500 ps, MD was performed at different temperatures, a comparison with the starting position of oxygen ions is presented in Fig. 10. In order to obtain a clearer view, a slice of oxygen ionic locations in the center of *Z* axes are marked red (For interpretation of the references to color in this figure legend, the reader is referred to the web version of the article). The simulation results showed that migration of O^{2-} anion accelerated by ramping temperature, which reflects conductivity increasing in the experiment.

The calculated oxygen anion diffusion coefficients at 973 K and 1273 K with varying Gd_2O_3 concentration are shown in Fig. 11, respectively. It can be seen from Fig. 11 that oxygen diffusion coefficients, which deduced from MSD results, increased by co-doping with Gd_2O_3 up to 3 mol% at 973 K. However, the addition of Gd_2O_3 decreases the oxygen diffusion coefficients, as shown in Fig. 11, for the simulations at 1273 K. The effect of Gd_2O_3 co-doping on enhancement of YSZ conduction only exhibits at the relatively low temperature, which is consistent with that observed in experiments. As mentioned above, co-doping YSZ with Gd_2O_3

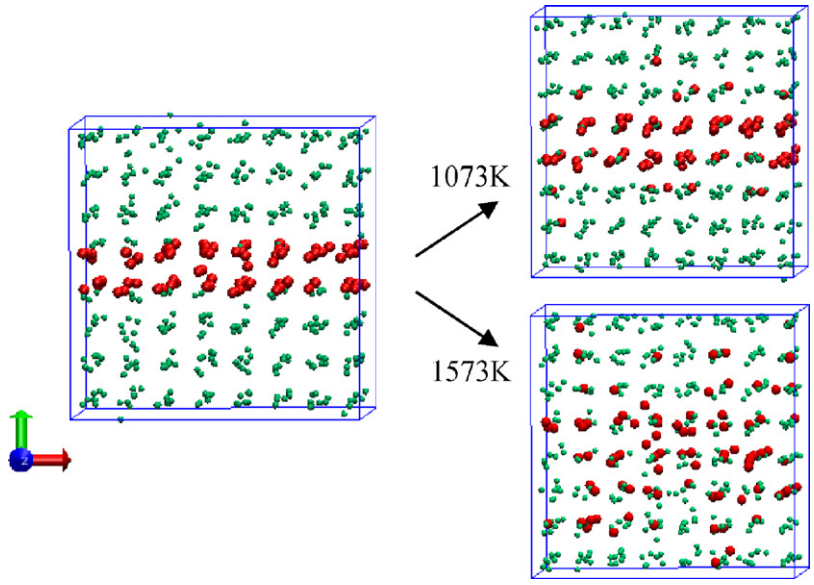

Fig. 10. The diffusion behavior of oxygen ions in electrolyte at 1073 K and 1573 K (a) before simulation and (b) after 500 ps simulation time.

can enhance conductivity due to its higher ordered cubic symmetry. However, this enhanced effect was marginalized with temperature ramping because the single cubic phase, from viewpoint of free energy, is likely to be more stable at higher temperatures than at lower temperatures. Therefore, YSZ is expected to have a higher conductivity than Gd_2O_3 co-doped specimens at an elevated temperature. It should be noted that the temperature employed in molecular dynamic simulation was higher than 973 K, because equilibrium state can hardly achieve even 500 ps simulation time for relaxation below 973 K.

4. Conclusions

This paper investigates the effect of Gd_2O_3 co-doping on the microstructure and ionic conductivity of YSZ electrolyte with a constant oxygen vacancy concentration. The molecular dynamics simulations were carried out to corroborate the results obtained from experiment and are generally in agreement with it. The YSZ bulk conductivity increased as the Gd_2O_3 content was increased up to 2 mol%, and decreased with further addition of Gd_2O_3 at low temperature (at constant vacancy concentration). The enhanced conductivity at low temperature was explained by the fact that Gd_2O_3 was more efficient in stabilizing the symmetry of the cubic phase. Moreover, Gd_2O_3 additions resulted in decreasing conductivity of grain boundary. The activation energy for the bulk conductivity was decreased with addition of Gd_2O_3, resulting in a lower conductivity of Gd_2O_3 doped samples at elevated temperature. It is also found that oxygen vacancies were preferentially located closer to Y^{3+} cation than Gd^{3+} cation in MD result.

Acknowledgements

This work was supported in part by a EPSRC studentship and Case studentship from Henson Ceramics Ltd. (LH). X Xie would also like to thank the China Scholarship Council for providing his exchange scholarship for Ph.D. study at the University of Cambridge.

References

[1] A. Rivera, J. Santamaria, C. Leon, Electrical conductivity relaxation in thin-film yttria-stabilized zirconia, Appl. Phys. Lett. 78 (2001) 610–612.
[2] J.S. Thokchom, H. Xiao, M. Rottmayer, T.L. Reitz, B. Kumar, Heterogeneous electrolyte ($YSZ–Al_2O_3$) based direct oxidation solid oxide fuel cell, J. Power Sources 178 (2008) 26–33.
[3] S.P. Jiang, Dependence of cell resistivity on electrolyte thickness in solid oxide fuel cells, J. Power Sources 183 (2008) 595–599.
[4] H. Gao, J. Liu, H. Chen, S. Li, T. He, Y. Ji, J. Zhang, The effect of Fe doping on the properties of SOFC electrolyte YSZ, Solid State Ionics 179 (2008) 1620–1624.
[5] J.T.S. Irvine, J.W.L. Dobson, T. Politova, S.G. Martin, A. Shenouda, Co-doping of scandia–zirconia electrolytes for SOFCs, Faraday Discuss. 134 (2007) 41–49.
[6] Y. Liu, L.E. Lao, Structural and electrical properties of ZnO-doped 8 mol% yttria-stabilized zirconia, Solid State Ionics 177 (2006) 159–163.
[7] M. Kurumada, H. Hara, E. Iguchi, Oxygen vacancies contributing to intragranular electrical conduction of yttria-stabilized zirconia (YSZ) ceramics, Acta Mater. 53 (2005) 4839–4846.
[8] J.A. Kilner, Meeting on Atomic Transport and Defect Phenomena in Solids, Royal Soc Chemistry, Guildford, England, 2006.
[9] R. Krishnamurthy, D.J. Srolovitz, K.N. Kudin, R. Car, Effects of lanthanide dopants on oxygen diffusion in yttria-stabilized zirconia, J. Am. Ceram. Soc. 88 (2005) 2143–2151.
[10] T.I. Politova, J.T.S. Irvine, Investigation of scandia–yttria–zirconia system as an electrolyte material for intermediate temperature fuel cells – influence of yttria content in system $(Y_2O_3)x(Sc_2O_3)(11-x)(ZrO_2)89$, Solid State Ionics 168 (2004) 153–165.
[11] M.S. Khan, M.S. Islam, D.R. Bates, Cation doping and oxygen diffusion in zirconia: a combined atomistic simulation and molecular dynamics study, J. Mater. Chem. 8 (1998) 2299–2307.
[12] Y. Kan, S. Li, P. Wang, G.-J. Zhang, O. Van der Biest, J. Vleugels, Preparation and conductivity of $Yb_2O_3–Y_2O_3$ and $Gd_2O_3–Y_2O_3$ co-doped zirconia ceramics, Solid State Ionics 179 (2008) 1531–1534.
[13] W. Smith, T. R. Forester, http://www.ccp5.ac.uk/DL_POLY/DL_POLY. Molecular simulation routines (The Council for the Central Laboratory of the Research Councils, Daresbury Laboratory, Daresbury, Nr. Warrington).
[14] M. Kilo, C. Argirusis, G. Borchardt, R.A. Jackson, Oxygen diffusion in yttria stabilised zirconia – experimental results and molecular dynamics calculations, PCCP 5 (2003) 2219–2224.
[15] G.V. Lewis, C.R.A. Catlow, Potential models for ionic oxides, J. Phys. C: Solid State Phys. 18 (1985) 1149–1161.
[16] M. Kilo, T. Homann, T. Bredow, Molecular dynamics calculations of anion diffusion in nitrogen-doped yttria-stabilized zirconia, Philos. Mag. 87 (2007) 843–852.
[17] L. Ping, I.W. Chen, E.P.-H. James, Effect of dopants on zirconia stabilization—an X-ray absorption study: III. Charge-compensating dopants, J. Am. Ceram. Soc. 77 (1994) 1289–1295.
[18] R.J. Darby, I. Farnan, R.V. Kumar, Delta the effect of co-doping on the yttrium local environment and ionic conductivity of yttria-stabilised zirconia, Ionics 15 (2009) 183–190.